Received: 25 March 2020 | Accepted: 22 July 2020
DOI: 10.1111/jvim.15868

STANDARD ARTICLE

Journal of Veterinary Internal Medicine Open Access
ACVIM American College of Veterinary Internal Medicine

A deletion of *IDUA* exon 10 in a family of Golden Retriever dogs with an attenuated form of mucopolysaccharidosis type I

Kiterie M. E. Faller[1,6] | Alison E. Ridyard[1] | Rodrigo Gutierrez-Quintana[1] | Angie Rupp[1] | Celia Kun-Rodrigues[2,7] | Tatiana Orme[2] | Karen L. Tylee[3] | Heather J. Church[3] | Rita Guerreiro[4,5,7] | Jose Bras[4,5,7]

[1]School of Veterinary Medicine, College of Medical, Veterinary, and Life Sciences, University of Glasgow, Glasgow, United Kingdom

[2]Department of Molecular Neuroscience, Institute of Neurology, University College London, London, United Kingdom

[3]Willink Biochemical Genetics Unit, Manchester Centre for Genomic Medicine, Manchester University NHS Foundation Trust, St Mary's Hospital, Manchester, United Kingdom

[4]Department of Neurodegenerative Diseases, Institute of Neurology, University College London, London, United Kingdom

[5]UK Dementia Research Institute at UCL (UK DRI), London, United Kingdom

[6]Royal (Dick) School of Veterinary Studies, The University of Edinburgh, Midlothian, United Kingdom

[7]Center for Neurodegenerative Science, Van Andel Research Institute, Grand Rapids, Michigan

Correspondence
Kiterie M. E. Faller, Royal (Dick) School of Veterinary Studies, The University of Edinburgh, Roslin, Midlothian, EH25 9RG, United Kingdom.
Email: kiterie.faller@ed.ac.uk

Funding information
Alzheimer's Society; University of Glasgow Small Animal Hospital Fund

Abstract

Background: Mucopolysaccharidosis type I (MPS-I) is a lysosomal storage disorder caused by a deficiency of the enzyme α-L-iduronidase, leading to accumulation of undegraded dermatan and heparan sulfates in the cells and secondary multiorgan dysfunction. In humans, depending upon the nature of the underlying mutation(s) in the *IDUA* gene, the condition presents with a spectrum of clinical severity.

Objectives: To characterize the clinical and biochemical phenotypes, and the genotype of a family of Golden Retriever dogs.

Animals: Two affected siblings and 11 related dogs.

Methods: Family study. Urine metabolic screening and leucocyte lysosomal enzyme activity assays were performed for biochemical characterization. Whole genome sequencing was used to identify the causal mutation.

Results: The clinical signs shown by the proband resemble the human attenuated form of the disease, with a dysmorphic appearance, musculoskeletal, ocular and cardiac defects, and survival to adulthood. Urinary metabolic studies identified high levels of dermatan sulfate, heparan sulfate, and heparin. Lysosomal enzyme activities demonstrated deficiency in α-L-iduronidase activity in leucocytes. Genome sequencing revealed a novel homozygous deletion of 287 bp resulting in full deletion of exon 10 of the *IDUA* gene (NC_006585.3(NM_001313883.1):c.1400-76_1521+89del). Treatment with pentosan polyphosphate improved the clinical signs until euthanasia at 4.5 years.

Conclusion and Clinical Importance: Analysis of the genotype/phenotype correlation in this dog family suggests that dogs with MPS-I could have a less severe phenotype than humans, even in the presence of severe mutations. Treatment with pentosan polyphosphate should be considered in dogs with MPS-I.

KEYWORDS
Hurler, iduronidase, lysosomal storage disease, Scheie

Abbreviations: GAGs, glycosaminoglycans; H&E, hematoxylin and eosin; LFB, Luxol fast blue; MPS, mucopolysaccharidosis; PAS, periodic acid-Schiff stain.

This is an open access article under the terms of the Creative Commons Attribution-NonCommercial License, which permits use, distribution and reproduction in any medium, provided the original work is properly cited and is not used for commercial purposes.
© 2020 The Authors. *Journal of Veterinary Internal Medicine* published by Wiley Periodicals LLC. on behalf of American College of Veterinary Internal Medicine.

1 | INTRODUCTION

Mucopolysaccharidoses (MPS) are a group of inherited lysosomal storage disorders (LSDs) characterized by a deficit in lysosomal enzymes necessary for the catabolism of glycosaminoglycans (GAGs). Accumulation of undegraded or partly degraded GAGs in the cells results in progressive multiple organ involvement. To date, deficiencies in 11 lysosomal enzymes have been identified, leading to 7 different subtypes of MPS.[1] These share common clinical features, although the degree of severity varies between, but also within, each MPS subtype. The most frequent findings include coarse facial features, a short stature, progressive skeletal disorders, organomegaly, corneal clouding and progressive neurological signs.[1,2]

MPS type I is the most frequent form of MPS, affecting 1 in 100 000 live births. It occurs secondary to a deficiency in the lysosomal enzyme α-L-iduronidase, leading to the accumulation of dermatan sulfate and heparan sulfates. It has historically been classified in 3 syndromes depending on the severity of the clinical signs, although overlap exists between this spectrum of phenotypes. Although recent therapies can improve life expectancy, quality of life, or both, there is still no cure for these disorders and alternative treatments remain desperately needed. For this, animal models of the disease have been playing a crucial role in the better understanding of the pathophysiology of the disease and in the development of advanced therapies.

Various naturally occurring forms of MPS have been described in veterinary medicine including in the dog (MPS I, II, IIIA, IIIB, VI, VII),[3-9] cat (MPS I, VI, VII),[10-12] farm animals (MPS IIIB and IIID),[13,14] and emus (MPS IIIB)[15]; research colonies have been established for some of MPS subtypes and are currently used as animal models of their human counterparts.[16,17]

We describe here the clinicopathologic findings of naturally occurring MPS-I in a Golden Retriever family, which we found to be caused by a full deletion of exon 10 of the gene coding for alpha-L-iduronidase (*IDUA*).

2 | MATERIAL AND METHODS

2.1 | Animal cases and ethical statement

The proband was presented to the University of Glasgow Small Animal Hospital for chronic diarrhea, weight loss and dysmorphism. Diagnostic investigations were performed as part of clinical procedures. A female littermate of the proband had previously been presented to the same institution for orthopedic signs and dysmorphism, for which no diagnosis was achieved, and she was soon thereafter euthanized at her owner request and no necropsy was performed. The breeder of the affected dogs and the owners of related dogs were contacted and agreed to provide DNA samples (cheek swabs) and pedigree information from their animals (Figure 1). The study was approved by the local ethical committee (University of Glasgow, School of Veterinary Medicine—Form ref 55a/15).

2.2 | Clinical investigations

Routine investigations included CBC, routine blood biochemistry, urinalysis, fecal culture, and diagnostic imaging tests (abdominal and cardiac ultrasound examinations and thoracic radiographs).

2.3 | Urinary metabolic studies and leucocyte lysosomal enzyme activities

Glycosaminoglycans were measured in the urine of the proband and a normal control dog for comparison. Urinary glycosaminoglycan concentration was determined using a colorimetric protocol as previously described.[18] Briefly glycosaminoglycans (GAGs) form complex molecules in the presence of the dye 1,9-dimethylmethylene blue (Sigma, UK) in acid solution. This produces a color change from blue to pink, which can be quantified at 520 nm against a standard of known concentration. Extracted GAGs were analyzed by 2-dimensional electrophoresis on cellulose acetate membranes and then visualized by staining with 0.05% alcian blue stain (Sigma, UK) to differentiate sulfated glycosaminoglycan patterns as previously described.[19]

Oligosaccharide and sialic acid analysis of urine was performed by thin layer chromatography (TLC) using a previously published protocol.[20] Urine oligosaccharides were separated on thin layer slica gel plates using a mobile phase of butanol/acetic acid/water (ratio 2 : 1 : 1) and then visualized by 0.2% orcinol and heat 100°C. Urine sialic acids were separated on thin layer slica gel plates using an initial mobile phase of butanol/acetic acid/water (ratio 2 : 1 : 1) followed by propan-1-ol/nitromethane/water (ratio 5 : 4 : 3) and then visualized by 0.2% recorcinol and heat 100°C.

The activities of lysosomal enzymes were measured in leucocytes from the proband and a normal control dog using commercially available 4-methylumbelliferyl substrates (Glycosynth, UK). The activity of α-L-iduronidase was measured in leucocytes using 2 mM 4-methylumbelliferyl-α-L-iduronide (Glycosynth, UK) in 0.4 M formate buffer pH 3.5 containing 0.9% sodium chloride, using the previously published protocol.[21] Arylsulfatase B activity was measured in leucocytes with 4-methylumbelliferyl-sulfate (Glycosynth, UK) 5 mg/mL in 0.1 M acetate buffer pH 5.4 according to the previously published protocol.[22] The activity of β-glucuronidase was measured in leucocytes using the substrate 5 mM 4-methylumbelliferyl-β-D-glucuronide (Glycosynth, UK) in 0.1 M acetate buffer pH 4.0. Briefly sample lysate 10 μL was incubated with 20 μL substrate for 15 minutes at 37°C. The reaction was terminated by the addition of 0.2 M carbonate buffer pH 9.5.

For each assay all incubations were performed at 37°C, and in each case the liberated 4-methylumbelliferone (4-MU) was measured using a LS55 luminescence spectrophotometer set at emission wavelength 450 nm and excitation wavelength 360 nm (PerkinElmer), against a 4-methylumbelliferone standard of known concentration (Sigma). The total protein was measured in cell lysate supernatants using the standard Lowry total protein assay and all enzyme activities were expressed as nmol 4-MU generated/mg total protein/hour.

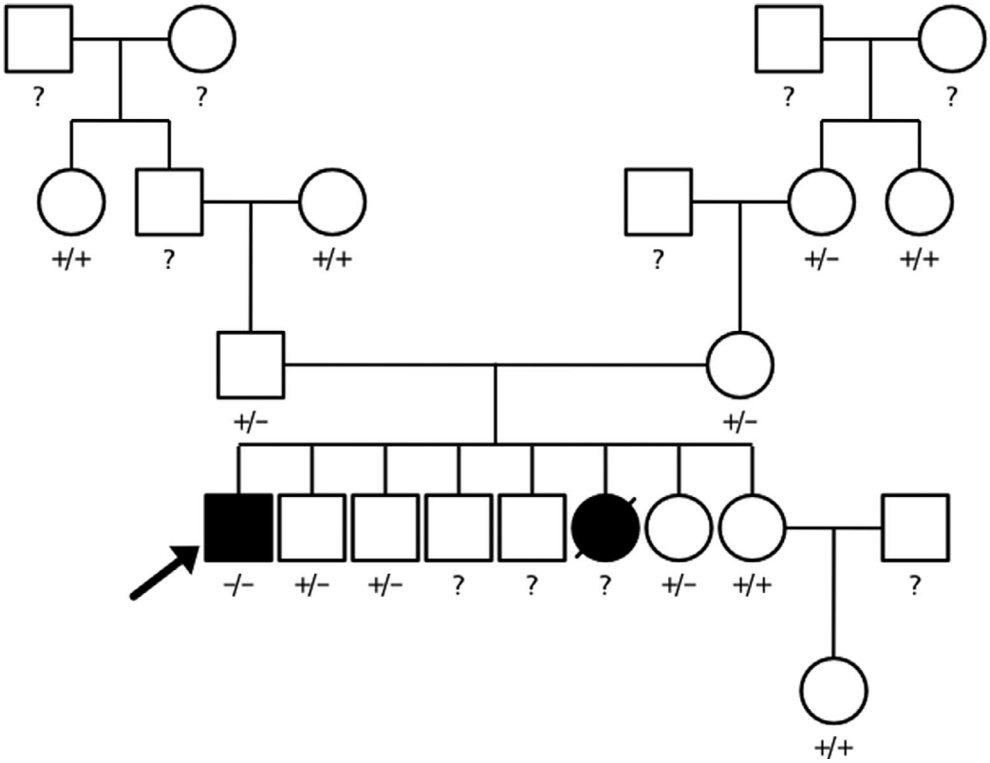

FIGURE 1 Pedigree of the affected dogs. Squares represent males and circle females. Affected individuals are depicted with the plain black symbols with the arrow highlighting the proband and black circle representing the suspected affected littermate (not genetically tested). Unaffected animals are represented with the white symbols. The genotype of the individuals is noted below each symbol: +/+ for dogs homozygous for the wild-type allele, +/− for heterozygous dogs, −/− for dogs homozygous for the variant lacking exon 10, and ? for nontested dogs

2.4 | Postmortem analysis

Following euthanasia, a full postmortem examination was performed. Representative samples from the lungs, spleen, kidney, urinary bladder, liver, heart and pericardium, adrenal gland, pancreas, thyroid, tongue, gastrointestinal tract, prostate, testis, skin, sciatic and vagus nerves, brain (multiple sections) and eye were fixed in 10% buffered formalin and snap frozen in isopentane chilled in liquid nitrogen. Slices of formalin-fixed samples were then routinely processed and embedded in paraffin before sectioning and staining with hematoxylin and eosin (H&E). Additionally, formalin-fixed tissue was also cut as frozen sections and stained with Oil Red O, Luxol fast blue (LFB) and periodic acid-Schiff stain (PAS).

2.5 | Molecular analysis

DNA from the affected animal was extracted from blood using a DNeasy Blood and Tissue kit (Qiagen, Crawley, UK). For the family relatives, DNA was extracted from cheek swabs using Gentra Puregene Buccal Cell Kit (Qiagen, Crawley, UK). Following PCR amplification (see Table S1), purification of the PCR products was performed using ExoSAP-IT (USB), before direct Sanger sequencing of both strands using BigDye Terminator v.3.1 chemistry v.3.1 (Applied Biosystems) and an ABI 3730XL Genetic Analyzer (Applied Biosystems). Sequencing traces were analyzed with Sequencher software v.4.2 (Gene Codes). However, due to the very high GC content of the region, some exons could not be amplified by PCR or Sanger sequencing (see Table S1) and whole-genome sequencing was then carried out by the Edinburgh Genomics laboratories, University of Edinburgh, using Illumina HiSeq X. Sequence alignment was performed against the dog genome reference CanFam3.1 using bwa[23] and the region corresponding to the *IDUA* gene was analyzed using IGV-Integrative Genome Viewer. The sequence has been deposited to the European Variant Archive under project ID PRJEB38456. Genotyping of family members was performed by PCR. Primers for PCR were as follow: Forward GCCACCGTGCTGCTCTAC; Reverse CATCCGACCACACCAAAAG. PCR was carried using a GC-RICH PCR system (Roche, Mannheim, Germany; Cat. No. 12140 306001) at the following reagent concentrations (200 μM each dNTP, 0.2 μM of each primer, 0.8 M GC-RICH resolution solution, 1X GC-RICH PCR Reaction buffer with DMSO [1.5 mM $MgCl_2$], and 1 U/25 μL of GC-RICH PCR System enzyme mix). Thermal cycling consisted of 5 minutes at 94°, followed by 20 touchdown cycles (94° for 15 seconds, 62°-0.5° at each cycle for 30 seconds, and 72° for 30 seconds), then followed by 10 further cycles (94° for 15 seconds, 52° for 30 seconds, and 72° for 30 seconds), and a final elongation stage of 72° for 5 minutes.

In addition, the genomes of 548 dogs from 107 dog breeds were screened for this specific variant[24] (see Table S2 for further information on the dog breeds).

3 | RESULTS

3.1 | Clinical history and examination

A 3 year and 6 month-old male Golden Retriever was presented to the Small Animal Hospital at the University of Glasgow with an

8-month history of diarrhea and weight loss and a long-standing history of dysmorphism. On presentation, the dog was alert and responsive but was markedly underweight (body condition score 2/9; body weight 21 kg). General examination revealed a dysmorphic appearance (Figure 2A); the proband was subjectively smaller than his littermates and had a disproportionately large head and tongue, prognathism, and a curved muzzle (Figure 2B). Excessive amount of soft tissue was also noted on the left caudal aspect of the tongue. On cardiac auscultation, a 1/6 systolic murmur with split S2 and occasional premature beats with pulse deficit were noted. The dog was also suffering from lipid deposits in both eyes (Figure 2C) and interdigital cysts between the fourth and fifth digits in all limbs (Figure 2D). Abnormal findings on neurological examination consisted in bilateral positional ventral strabismus and nystagmus (of variable direction). This dog originated from a litter of 8 puppies, of which a female littermate was euthanized a few months earlier. She exhibited similar dysmorphic changes and corneal lipid deposits; however, no diagnosis was achieved at that time. In both dogs, abnormal limb conformation was first noted by the breeder from the age of 3 to 4 months, and in the euthanized bitch multiple joint laxities (carpi and stifles) were noted by a veterinary orthopedic surgeon when she was 9 months old.

3.2 | Clinical investigations

No abnormality was detected on routine CBC. Abnormalities in serum biochemistry profile included a mildly decreased albumin (2.6 g/dL—reference interval [RI]: 2.9-3.6), a moderately raised urea (93 mg/dL—RI: 15-51; 15.5 mmol/L—RI: 2.5-8.5) with normal creatinine and a raised alanine aminotransferase (ALT) (371 IU/L—RI: <90 IU/L). Serum trypsin-like immunoreactivity (TLI), folate, cobalamin, adrenocorticotropic hormone (ACTH) stimulation test, thyroid function tests (TT4 and cTSH) were within normal limits. Urinalysis showed a urinary specific gravity of 1.032, presence of microscopic blood and a urinary protein to creatinine ratio of 0.36 (normal <0.2; 0.2 to 0.5 is considered borderline proteinuric[25]). Fecal culture detected the presence of *Campylobacter upsaliensis* of unknown/questionable clinical relevance. Thoracic radiographs did not reveal any substantial abnormality with the exception of a mild generalized osteopenia and mild vertebral changes (Figure 3C). Abdominal ultrasonography showed a hepatosplenomegaly, absence of a left kidney and presence of sediment/small calculi within the urinary bladder.

Echocardiography revealed severe thickening of mitral valve leaflets, all aortic leaflets and the tricuspid septal leaflet (Figure 3A,B). A left ventricular diastolic dysfunction was diagnosed based on presence of mitral inflow and abnormal relaxation pattern on the tissular Doppler imaging (TDI). Systolic function was adequate (fractional shortening 29%: reference interval: 27-55).[26]

3.3 | Biochemical confirmation of diagnosis

Quantification of urinary oligosaccharides and sialic acid was within normal limits.

Urinary glycosaminoglycan analysis revealed a marked increase in concentrations of dermatan and heparan sulfates (Figure S1).

The activities of the relevant lysosomal enzymes are shown in Table 1. The marked deficiency in α-L-iduronidase activity, reduced to 1.3% of the normal control dog activity, was consistent with a diagnosis of MPS-I. Since a biochemical diagnosis of MPS-I had been established, the activity of iduronate-2-sulfatase was not measured.

3.4 | Treatment and outcome

Initial symptomatic treatment for the chronic weight loss and diarrhea consisted in a 2-week course of amoxicillin/clavulanate (Synulox, Zoetis UK) and a dietary change to a hydrolyzed diet (Purina HA, Nestlé Purina Petcare), which resulted in a resolution of the diarrhea and an improvement in demeanor. Following diagnosis of MPS-I, supplementation with pentosan polyphosphate (PPS) (Cartrophen Vet 100 mg/mL solution for Injection, Biopharm Australia; 3 mg/kg weekly subcutaneous injections) was started and resulted in subjective improvement in pelvic limb strength. Due to the possible interference of PPS with the coagulation pathways, coagulation times were monitored but remained within normal limits. Cardiac function was reevaluated 3 months after the first scan and showed similar valvular changes but a worsening of the systolic function (fractional shortening: 15%). Nine months after initial presentation, the dog's quality of life deteriorated; he had become more exercise intolerant and weaker. Body weight had decreased to 20.4 kg. Infection of the interdigital cysts resulted in left forelimb lameness; neurological examination was unchanged. The owner elected for euthanasia when the dog was 4.5 years old.

3.5 | Gross, histopathological, and immunohistochemical findings

Gross postmortem examination confirmed previously identified abnormalities in the live dog, the most relevant ones being follicular cysts between digits 4 and 5, the bilateral corneal deposits, the lack of a left kidney (with presence of a blind-ending left ureter), the hepatomegaly and the firm growth extending from the ventral oral mucosa on the left side of the tongue. All cardiac valves were thickened, with such changes more pronounced in the atrioventricular valves of both sides when compared to the semilunar valves (Figure 4A). Bilaterally, the vagus nerves appeared thickened and firm. The prostate gland was symmetrically and mildly to moderately enlarged.

The histological changes were consistent with a common pattern of accumulation of myxomatous material and fibrosis. These myxomatous changes were most evident in all heart valves, the presumed vagus nerves (histologically no nervous tissue was appreciable anymore), parts of the sciatic nerve and predominantly the tunica intima, less so the tunica media of large vessels, whereas fibrosis was evident in the pulmonary pleura, the pericardium, the epicardium, the leptomeninges, the adrenal cortex and also the medulla of the peripheral

FIGURE 2 Photographs of the proband. A, Note the generalized muscle wastage. B, Facial dysmorphism was apparent with a curved muzzle highlighted by the red line drawn above. Mandibular prognatism was also evident. C, Lipidic corneal deposits, which were present bilaterally. D, Interdigital follicular cyst

lymph node examined. Numerous organs, including the spleen, kidney, urinary bladder, liver, gastrointestinal system, lymph nodes, skin, nerves, leptomeninges, cornea, and also the collagenous tissue forming growths extending from the tongue and overlying the epicardium contained foamy macrophages (Figure S2). Additionally, numerous cells, including tubular epithelial cells, urothelial cells, biliary and pancreatic ductular epithelium, apocrine gland epithelium, adrenal cortical cells, hepatocytes, smooth muscle myofibres of large heart and mesenteric arteries, Leydig (interstitial) cells, Schwann cells/myelin and neurons appeared vacuolated. More specifically, well-appreciable cytoplasmic vacuolation was observed in individual neurons of the temporal, occipital and frontal cortex, large neurons of the caudate nucleus and neurons of the caudal colliculi, and in larger numbers of neurons of the thalamic nuclei, lateral and medial geniculate nuclei, the Purkinje cells (Figure 5B) and ventral horn nuclei. However, no appreciable vacuolation was observed in neurons of the piriforme lobe, the hippocampus, the rostral colliculi, the pontine nuclei, the dorsal horn and autonomic ganglia. In addition to the neuronal vacuolation, the most prominent histological changes observed in the brain consisted in a moderate to marked diffuse Purkinje cell loss of the cerebellum (Figure 5A).

Staining of vacuolated cells with Oil Red O, PAS, Toluidine Blue and LFB was inconsistent both on routinely processed and frozen sections of fixed tissue. With Oil Red O, cytoplasmic staining of the macrophages in the spleen (Figure S2), but no other organ was observed, while with PAS and LFB, renal, splenic and leptomeningeal macrophages and also cortical neurons, Purkinje cells (Figure 5C,D) and neurons of the medulla oblongata variably exhibited a cytoplasmic stain. With Toluidine Blue, some macrophages in the vagus nerve stained. The vacuolated myofibres of large vessels and vacuolated hepatocytes throughout failed to be stained by special stains even when conducted on frozen sections.

Staining with Alcian Blue was more consistent and confirmed the deposition of myxomatous material observed both grossly and histologically in large vessels, large nerves and heart valves. Macrophages in the spleen and cerebral leptomeninges also contained mildly Alcian Blue-positive foamy material. Sciatic and vagus nerves showed multifocal (sciatic; Figure 4C) to diffuse (vagus) myxomatous degeneration, with replacement of the axons and Schwann cells by myxomatous ground substance (Alcian Blue positive) and foamy macrophages.

The polypoid growth extending from the left ventral aspect of the tongue consisted of large amounts of poorly to moderately cellular

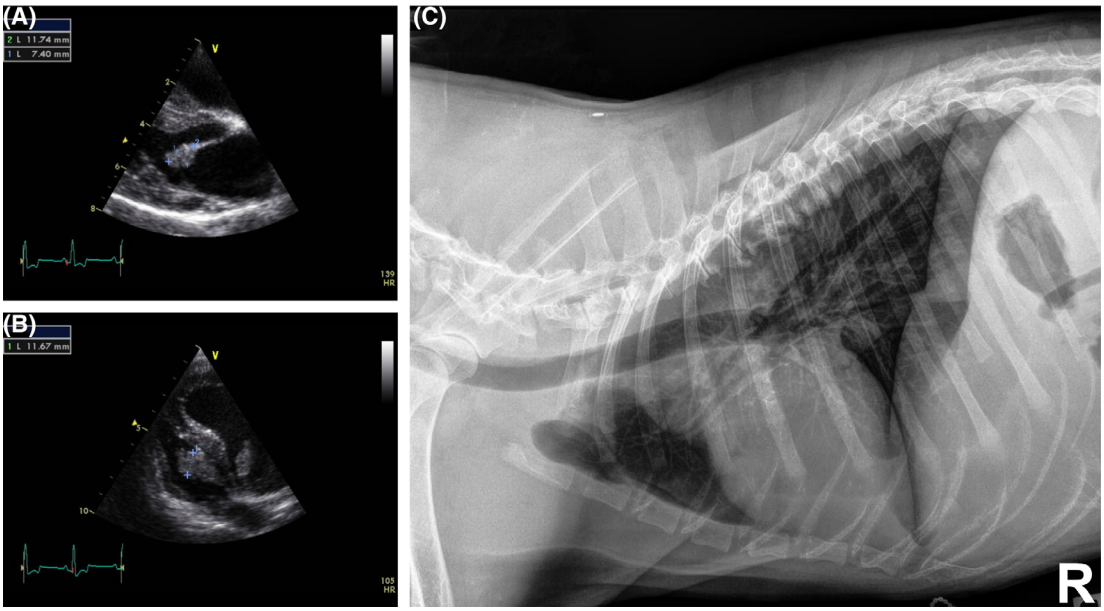

FIGURE 3 Echocardiographic and radiographic findings. A, Right parasternal long axis image showing marked thickening of the septal mitral valve leaflet (cursors). B, Left parasternal 4-chamber image showing marked thickening of the septal tricuspid valve leaflet (cursor). C, Right lateral thoracic radiograph. Note the midthoracic spondylosis with possible fusion of T5/T6 and the irregular shape of T6/T7 endplates. There is a mild decrease in bone density along the vertebrae with some thinning of the humeral cortices

TABLE 1 Activities of the relevant lysosomal enzymes measured in the leucocytes of the affected dog compared to a normal control dog and a normal human population

		Enzyme activity (nmol/mg/h)		
Enzyme	Disorder	Affected dog	Control dog	Human reference range
α-L-Iduronidase	MPS I	0.07	5.2	10-50
Arylsulfatase B	MPS VI	10	7	>5
β-Glucuronidase	MPS VII	130	169	100-800

Note: A marked deficiency in α-L-iduronidase was observed, consistent with a diagnosis of MPS-I.

collagen reminiscent of a (early) collagenous hamartoma. Other main histological abnormalities comprised a marked diffuse centrilobular hepatocellular lipidosis and a moderate, multifocal, chronic cortical fibrosis of the right kidney. Although a left ureter was present, there was no evidence of kidney tissue on that side. The seminiferous tubules of the testicles multifocally exhibited a marked reduction in number of spermatogonia; overall, only few spermatids were seen. The interstitial Leydig cells were also vacuolated (Figure 4D). Finally, histological changes consistent with prostatic hyperplasia were observed.

3.6 | Genetic analysis

We initially aimed to sequence all exons of the *IDUA* gene by Sanger sequencing. Exons 1 to 8, 13 and 14 did not show any variant compared to the dog reference genome (CanFam3.1). A synonymous variant was detected in exon 12. Amplification of the region containing exons 10 to 11 strongly suggested a homozygous deletion of the entire exon 10. However, as exon 9 could not be amplified and taking in consideration the overall extremely high GC content of the whole region of the *IDUA* gene, it was decided to proceed to a full genome sequencing to prove the authenticity of the deletion and for better identification of the deletion boundaries. Whole genome sequencing confirmed a 287 bp homozygous deletion resulting in the full deletion of exon 10 (NC_006585.3(NM_001313883.1):c.1400-76_1521+89del); NC_006585.3:g.91523238_91523524del (Figure 6). Amplification of this region by PCR in the available relatives confirmed segregation of the mutation within the family with both unaffected parents being heterozygous for the mutation (Figure 1).

This large deletion is predicted to result in a frame shift leading to a change in protein sequence from amino acid 468 and a truncated protein due to a premature codon stop (528 aa vs 655) (NP_001300812.1:p.(Gly467_Glu507del)). We also screened a large population of 548 dogs of various breeds for this variant (Table S2). The variant was not found in any of the analyzed dog genomes.

4 | DISCUSSION

In this study, we describe a Golden Retriever family affected by MPS-I secondary to a full deletion of the *IDUA* exon 10. The proband

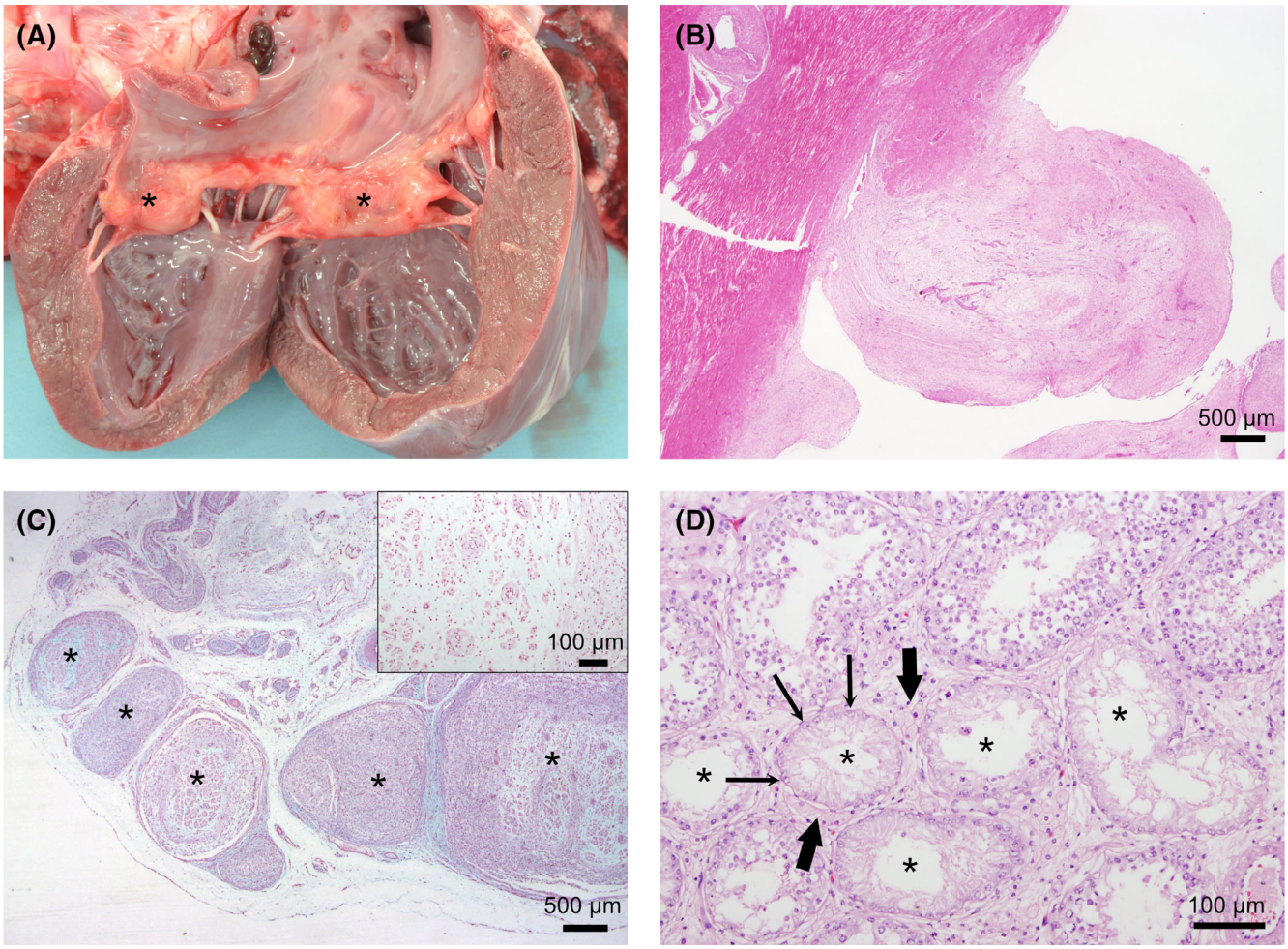

FIGURE 4 Pathological findings. A, Gross pathology of the heart. Note the moderately to markedly thickened mitral valves (asterisks). B, Light microscopic view of a section through the thickened mitral valves. H&E stain. C, Light microscopic view of a transverse section of the sciatic nerve (major fascicles marked with asterisks). Alcian Blue stain. There is moderate accumulation of interstitial myxomatous material combined with a conspicuous dispersion and loss of myelinated nerve fibers. The inset show a higher magnification of the sciatic nerve fascicle on the far right. D, Light microscopic view of a testicular section. H&E stain. Multifocally, the seminiferous tubes exhibit a marked hypocellularity (asterisks), interpreted to represent a lack of spermatogonia of all stages with a preservation of Sertoli cells (thin arrows). The Leydig cells (thick arrows) throughout are vacuolated

presented with a chronic history of dysmorphism and recent gastrointestinal symptoms. The short stature and dysmorphism combined with the clinical findings of corneal deposits, hepatomegaly, and marked cardiac valvular changes was strongly suggestive of MPS. Diagnosis of MPS-I was confirmed by accumulation of dermatan and heparan sulfates in urine and low enzymatic activity of α-L-iduronidase in leucocytes.

Mucopolysaccharidoses are a group of inherited LSDs characterized by defective lysosomal enzymes, resulting in progressive accumulation of GAGs in the cells of various tissues.[1,27] Identification of elevated urinary GAGs is a useful screening test; however, as dermatan sulfate and heparan sulfate also accumulate in MPS II, VI and VII, confirmatory diagnosis of MPS is typically obtained by testing enzyme activity in leucocytes (in this case α-L-iduronidase). Once a diagnosis is obtained, molecular characterization of the mutation can be performed. Here, characterization of the mutation was initially sought by Sanger sequencing the *IDUA* gene. However, considering the extremely high GC content of the region (over 80% for some exons), PCR amplification of 1 of the exons could not be achieved. Moreover, as we could not completely exclude—although very unlikely—that the strongly suspected full deletion of exon 10 could be an artifact due to the high GC content of the region, we confirmed the deletion by using another sequencing technique (whole genome sequencing). We identified a new mutation, which affects the reading frame from amino acid 468 and is predicted to result in a truncated mutant protein of 528 amino acids, with modification/loss of the last 187 amino acids of the normal protein. However, these predictions need to be considered carefully without further analysis of the mRNA transcript or protein. Indeed, we cannot exclude for the aberrant transcript to be quickly degraded or for alternative splicing to occur. Although at this stage the prevalence of this mutation in the Golden Retriever breed remains unknown, screening before breeding could

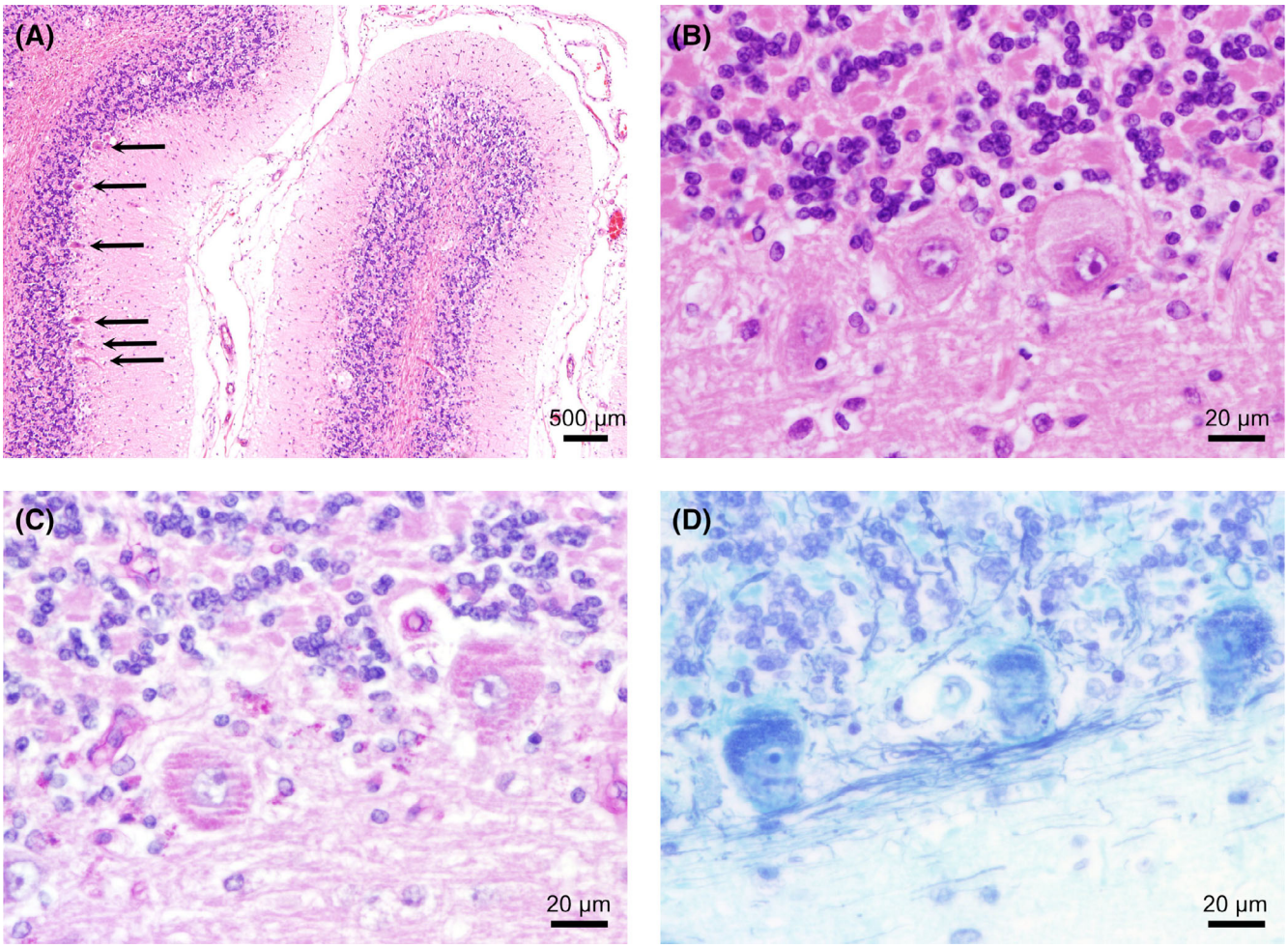

FIGURE 5 Light microscopic images of the cerebellum. A, There is a moderate to marked decrease in the number of Purkinje cells (arrows). Low magnification. H&E stain. B, At higher magnification, many of the remaining Purkinje cells exhibit fine intracytoplasmic vacuoles (H&E stain), which stain positive with periodic acid-Schiff (PAS), C and Luxol fast blue (LFB), D

be considered to progressively eradicate this variant from the population.

The histological findings were in line with those previously described in the animal models of MPS-I (ie, the Plott Hound dog model,[7,28] the feline model,[29] and the genetically engineered murine knock-out model[30]) as well as those described in affected humans.[31] Staining of the storage material with PAS, Alcian Blue and Toluidine Blue proved to be variable and inconsistent, in line with previous reports in various types of MPS.[7,15,32-34] This could be attributed to the heterogeneity of the storage material,[15,34] the water-solubility of GAGs[4,31] and to the fact that the staining of mucins is overall very variable depending on their degree of acidity.[35,36]

In humans, MPS-I (OMIM #252800) is the most frequent form of MPS but remains overall a rare syndrome with a prevalence of 1 in 100 000 live births.[37] Depending upon the severity of the clinical signs, age at onset and life expectancy, 3 forms have been historically defined.[37,38] Hurler syndrome (MIM #607014) is the most severe form with a diagnosis usually made within the first year of life. Typical signs include coarsening of facial features, progressive skeletal dysplasia, hepatosplenomegaly, corneal clouding, marked cardiac valvular changes and severe intellectual disability. Death frequently occurs within the first 10 years of life due to cardiorespiratory failure secondary to cardiac arrhythmias, or coronary artery disease. In the mildest form of MPS-I, also known as Scheie syndrome (MIM #607016), patients have normal or near normal intellectual capabilities, but frequently suffer from cardiac, ophthalmological and skeletal malformations. These patients usually have a near normal life expectancy. An intermediate form is referred to as Hurler-Scheie syndrome (MIM #607015), with affected patients typically surviving to adulthood.[37-39] Nowadays, it is acknowledged that these 3 forms represent a continuous spectrum of clinical signs, with no strict biochemical or molecular diagnostic criteria available to separate them[4,38,40-42]; consequently, individuals are more and more classified into severe (Hurler) and attenuated (Hurler-Scheie, Scheie) forms.[38] Although some degree of genotype–phenotype correlation is established for the most frequently observed variants, it remains difficult to predict the effect of the more "unique" mutations.[38,41] While patients with a nonsense mutation on both alleles will almost invariably develop a

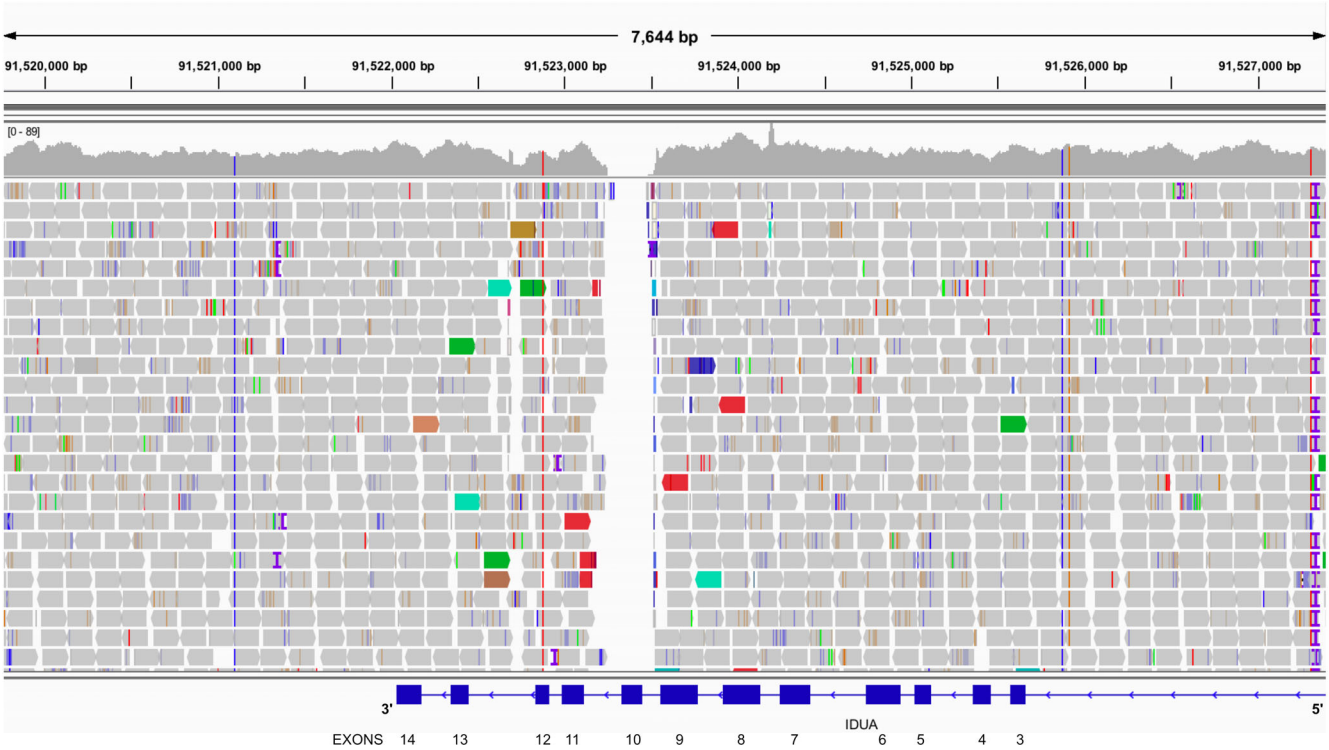

FIGURE 6 Integrated Genomics Viewer (IGV) display of the 3′ end of the IDUA gene sequencing data of the affected dog. The lower panel of the display shows the normal structure of the gene with the location of exons 3 to 14. In the affected dog, there is a deletion of the entire exon 10

severe phenotype, the effects of less severe mutations, such as amino acid substitutions, are more difficult to prognosticate.[43] More work is being done in that field of genoype-phenotype correlation including trying to predict the effect of "private" mutations using in silico tools such as independent function prediction scores and ensemble scores.[44-46] This is particularly important as most of the identified mutations are "unique" and estimating the effect of a mutation on the phenotype of a newborn child has relevant consequences in terms of therapeutic options.[43,44,47] Over 200 pathogenic variants are currently indexed on the Human Gene Mutation database. Most variants are single point mutations[48] and until recently, no whole exon or full gene deletion had been described.[46,49] Therefore, when looking for new mutations in a human patient, the possibility of a full exon deletion should be borne in mind especially when determining the most suitable technique for genetic analysis. Some of these mutations, homozygous deletions in particular, could be missed by Sanger sequencing and a combination of methods may be required.[50]

In the family of dogs presented here, a full deletion of exon 10 was identified. This leads to a phenotype of similar severity to that presented by the well-characterized Plott Hound dog model of MPS-I, which is due to a G > A transition in the splicing site of intron 1, leading to the retention of the intron and creation of a premature stop codon.[51] In both dog models, the phenotype resembles more closely to the human intermediate/attenuated form of MPS-I. The first abnormality detected by the breeder of the dogs presented here was an abnormal limb conformation and a stunted growth, which was first noted by the age of 3 to 4 months. The main clinical signs were skeletal, cardiac and ocular as seen in the Plott Hound model.[52] Facial changes were also striking with a curved muzzle typically seen in affected dogs[53] and a mandibular prognatism, also described in humans.[54] Moreover, while no marked behavioral change was identified by the owner or the clinician, subtle neurological signs were detected on neurological examination. Finally, the dog also reached reproductive age. In human patients with 2 null variants of *IDUA* such as a nonsense mutation or a large deletion, a severe phenotype is consistently observed.[43,46] This would suggest that the phenotype in the dog models is attenuated compared to what would be expected in humans suffering from nonsense mutations. A similar phenotype attenuation has been discussed in the murine knock-out[30] and spontaneous feline model,[29] which also reached adulthood. This is an interesting finding highlighting the limitations of animal models, which do not always fully reproduce the human phenotype. The reason why these animals do not suffer from a severe form remains unknown and could be due to subtle variations in the metabolic rate of GAG depending on the species.[30] Understanding these interspecies differences could be an interesting subject of research, for which the establishment of a new dog research colony from these Golden retriever dogs could prove helpful.

The main concern of the proband's owner was the recent onset of gastrointestinal signs. Episodic diarrhea is also seen in many children with Hurler's disease. Its etiology remains unknown although abnormal intestinal flora has been suggested.[55] The proband also

suffered from renal agenesis. To the best of our knowledge, this has never been described in people suffering from MPS-I and in this case very likely represents an incidental and unrelated finding. However, we cannot fully exclude that this could be a previously unseen sign. Interestingly, histopathology revealed testicular changes, which is poorly documented in people with MPS although testicular histopathological changes were observed in a 19 year old man suffering from MPS-II.[56] Recently, male reproductive function was assessed in a murine model of MPS-I. In these mice, tubular degeneration and disorganization of the seminiferous epithelium with tubules containing very few germ cells were observed histologically, similar to the findings observed in this dog. Consistent with the histological findings, these mice exhibited a marked reduction in the daily sperm production but the plasma testosterone concentrations remained normal.[57] The fact that testosterone concentrations remain unchanged would explain the benign prostatic hyperplasia seen in the proband.

Animal models of MPS-I have played an important role in the development of therapies in humans. However, although hematopoietic stem cell transplant (HSCT) and enzyme replacement therapy (ERT) have improved the prognosis for these patients, there is still no cure and new therapies such as gene therapies are still desperately sought.[1,27,58-61] Dog models have been extremely valuable in the development of these therapies over the last 3 decades[62-67] and while generation of an *IDUA* knock-out mouse has certainly increased the speed of research and lowered the cost, studies on large animal models remain complementary. Larger animal models such as cats and dogs have a longer life expectancy, making it more appropriate to test therapeutics including their potential complications in the long term.[16,68] Their size and neuroanatomy (gyrencephalic vs lissencephalic brain) is also closer to that of a young child, allowing better assessment of more advanced treatment such as stereotaxic injections.[53,68,69] In the present case, the prohibitive cost of ERT precluded its use, all the more as weekly injections are typically required.[28] Experimental treatment with PPS has recently been shown to have a beneficial effect in the rat model of MPS-VI and dog model of MPS-I, resulting in a marked reduction of the associated-inflammation but also a reduction in the accumulation of GAG in the tissues and urine.[70-72] Although improvement of quality of life was reported by the owner of the current dog after the treatment was initiated, this remains subjective.

In conclusion, we have described a dog with MPS-I, which resembles the attenuated form of the human disease. In this dog, the disease is secondary to a full deletion of the exon 10 of the *IDUA* gene, leading to a deficiency in α-L-iduronidase activity. Contrary to what would be expected in human patients with such a severe mutation, the phenotype of this dog remained attenuated.

ACKNOWLEDGMENTS

We are grateful to the breeder and the owners of the dogs for contributing to this study. We thank the collaborators of the Dog Biomedical Variant Database Consortium (DBVDC), Gus Aguirre, Catherine André, Danika Bannasch, Doreen Becker, Cord Drögemüller, Kari Ekenstedt, Oliver Forman, Steve Friedenberg, Eva Furrow, Urs Giger, Christophe Hitte, Marjo Hytönen, Vidhya Jagannathan, Tosso Leeb, Hannes Lohi, Cathryn Mellersh, Jim Mickelson, Leonardo Murgiano, Anita Oberbauer, Sheila Schmutz, Jeffrey Schoenebeck, Kim Summers, Frank van Steenbeck, Claire Wade for sharing dog genome sequence data from control dogs.

CONFLICT OF INTEREST DECLARATION

Authors declare no conflict of interest.

OFF-LABEL ANTIMICROBIAL DECLARATION

Authors declare no off-label use of antimicrobials.

INSTITUTIONAL ANIMAL CARE AND USE COMMITTEE (IACUC) OR OTHER APPROVAL DECLARATION

Approved by the local ethical committee of the University of Glasgow, School of Veterinary Medicine, Form ref 55a/15.

HUMAN ETHICS APPROVAL DECLARATION

Authors declare human ethics approval was not needed for this study.

ORCID

Kiterie M. E. Faller https://orcid.org/0000-0002-4525-7059
Rodrigo Gutierrez-Quintana https://orcid.org/0000-0002-3570-2542

REFERENCES

1. Lampe C, Bellettato CM, Karabul N, Scarpa M. Mucopolysaccharidoses and other lysosomal storage diseases. *Rheum Dis Clin North Am*. 2013;39:431-455.
2. Tomatsu S, Fujii T, Fukushi M, et al. Newborn screening and diagnosis of mucopolysaccharidoses. *Mol Genet Metab*. 2013;110:42-53.
3. Ellinwood NM, Wang P, Skeen T, et al. A model of mucopolysaccharidosis IIIB (Sanfilippo syndrome type IIIB): N-acetyl-alpha-D-glucosaminidase deficiency in Schipperke dogs. *J Inherit Metab Dis*. 2003;26:489-504.
4. Fischer A, Carmichael KP, Munnell JF, et al. Sulfamidase deficiency in a family of Dachshunds: a canine model of mucopolysaccharidosis IIIA (Sanfilippo A). *Pediatr Res*. 1998;44:74-82.
5. Neer TM, Dial SM, Pechman R, Wang P, Oliver JL, Giger U. Clinical vignette. Mucopolysaccharidosis VI in a miniature pinscher. *J Vet Intern Med*. 1995;9:429-433.
6. Ray J, Bouvet A, DeSanto C, et al. Cloning of the canine beta-glucuronidase cDNA, mutation identification in canine MPS VII, and retroviral vector-mediated correction of MPS VII cells. *Genomics*. 1998;48:248-253.
7. Shull RM, Helman RG, Spellacy E, Constantopoulos G, Munger RJ, Neufeld EF. Morphologic and biochemical studies of canine mucopolysaccharidosis I. *Am J Pathol*. 1984;114:487-495.
8. Wilkerson MJ, Lewis DC, Marks SL, Prieur DJ. Clinical and morphologic features of mucopolysaccharidosis type II in a dog: naturally occurring model of Hunter syndrome. *Vet Pathol*. 1998;35:230-233.
9. Yogalingam G, Pollard T, Gliddon B, Jolly RD, Hopwood JJ. Identification of a mutation causing mucopolysaccharidosis type IIIA in New Zealand Huntaway dogs. *Genomics*. 2002;79:150-153.
10. Fyfe JC, Kurzhals RL, Lassaline ME, et al. Molecular basis of feline beta-glucuronidase deficiency: an animal model of mucopolysaccharidosis VII. *Genomics*. 1999;58:121-128.
11. He X, Li CM, Simonaro CM, et al. Identification and characterization of the molecular lesion causing mucopolysaccharidosis type I in cats. *Mol Genet Metab*. 1999;67:106-112.

12. Jezyk PF, Haskins ME, Patterson DF, Mellman W, Greenstein M. Mucopolysaccharidosis in a cat with arylsulfatase B deficiency: a model of Maroteaux-Lamy syndrome. *Science*. 1977;198:834-836.
13. Karageorgos L, Hill B, Bawden MJ, Hopwood JJ. Bovine mucopolysaccharidosis type IIIB. *J Inherit Metab Dis*. 2007;30:358-364.
14. Thompson JN, Jones MZ, Dawson G, Huffman PS. N-acetylglucosamine 6-sulphatase deficiency in a Nubian goat: a model of Sanfilippo syndrome type D (mucopolysaccharidosis IIID). *J Inherit Metab Dis*. 1992;15:760-768.
15. Palmieri C, Giger U, Wang P, Pizarro M, Shivaprasad HL. Pathological and biochemical studies of mucopolysaccharidosis type IIIB (Sanfilippo syndrome type B) in juvenile emus (*Dromaius novaehollandiae*). *Vet Pathol*. 2015;52:160-169.
16. Ellinwood NM, Vite CH, Haskins ME. Gene therapy for lysosomal storage diseases: the lessons and promise of animal models. *J Gene Med*. 2004;6:481-506.
17. Haskins ME. Animal models for mucopolysaccharidosis disorders and their clinical relevance. *Acta Paediatr*. 2007;96:56-62.
18. de Jong JG, Wevers RA, Liebrand-van Sambeek R. Measuring urinary glycosaminoglycans in the presence of protein: an improved screening procedure for mucopolysaccharidoses based on dimethylmethylene blue. *Clin Chem*. 1992;38:803-807.
19. Wessler E. Analytical and preparative separation of acidic glycosaminoglycans by electrophoresis in barium acetate. *Anal Biochem*. 1968;26:439-444.
20. Sewell AC. An improved thin-layer chromatographic method for urinary oligosaccharide screening. *Clin Chim Acta*. 1979;92:411-414.
21. Stirling JL, Robinson D, Fensom AH, et al. Fluorimetric assay for prenatal detection of Hurler and Scheie homozygotes or heterozygotes. *Lancet*. 1978;1:147.
22. Fluharty AL, Stevens RL, Sanders DL, Kihara H. Arylsulfatase B deficiency in Maroteaux-Lamy syndrome cultured fibroblasts. *Biochem Biophys Res Commun*. 1974;59:455-461.
23. Li H, Durbin R. Fast and accurate short read alignment with Burrows-Wheeler transform. *Bioinformatics*. 2009;25:1754-1760.
24. Jagannathan V, Drögemüller C, Leeb T, et al. A comprehensive biomedical variant catalogue based on whole genome sequences of 582 dogs and eight wolves. *Anim Genet*. 2019;50:695-704.
25. Bartges JW. Chronic kidney disease in dogs and cats. *Vet Clin North Am Small Anim Pract*. 2012;42:669-692. vi.
26. Morrison SA, Moise NS, Scarlett J, Mohammed H, Yeager AE. Effect of breed and body weight on echocardiographic values in four breeds of dogs of differing somatotype. *J Vet Intern Med*. 1992;6:220-224.
27. Wraith JE. Mucopolysaccharidoses and mucolipidoses. *Handb Clin Neurol*. 2013;113:1723-1729.
28. Kakkis ED, McEntee MF, Schmidtchen A, et al. Long-term and high-dose trials of enzyme replacement therapy in the canine model of mucopolysaccharidosis I. *Biochem Mol Med*. 1996;58:156-167.
29. Haskins ME, Aguirre GD, Jezyk PF, Desnick RJ, Patterson DF. The pathology of the feline model of mucopolysaccharidosis I. *Am J Pathol*. 1983;112:27-36.
30. Clarke LA, Russell CS, Pownall S, et al. Murine mucopolysaccharidosis type I: targeted disruption of the murine alpha-L-iduronidase gene. *Hum Mol Genet*. 1997;6:503-511.
31. Wolfe HJ, Blennerhasset JB, Young GF, et al. Hurler's syndrome: a histochemical study. New techniques for localization of very water-soluble acid mugopolysaccharides. *Am J Pathol*. 1964;45:1007-1027.
32. Zimmermann B 3rd, Lally EV, Sharma SC, et al. Severe aortic stenosis in systemic lupus erythematosus and mucopolysaccharidosis type II (Hunter's syndrome). *Clin Cardiol*. 1988;11:723-725.
33. Jolly RD, Allan FJ, Collett MG, Rozaklis T, Muller VJ, Hopwood JJ. Mucopolysaccharidosis IIIA (Sanfilippo syndrome) in a New Zealand Huntaway dog with ataxia. *N Z Vet J*. 2000;48:144-148.
34. Jolly RD, Johnstone AC, Norman EJ, Hopwood JJ, Walkley SU. Pathology of mucopolysaccharidosis IIIA in Huntaway dogs. *Vet Pathol*. 2007;44:569-578.
35. Layton C, Bancroft JD. Carbohydrates. In: Suvarna SK, Layton C, Bancroft JD, eds. *Bancroft's Theory and Practice of Histological Techniques*. 7th edition. Oxford: Churchill Livingstone Elsevier; 2013:215-238.
36. Rongioletti F, Rebora A. Mucinoses. In: Bolognia JL, Jorizzo JL, Schaffer JV, eds. *Dermatology*. 3rd edition. Philadelphia: Elsevier; 2012:687-698.
37. Muenzer J, Wraith JE, Clarke LA, International Consensus Panel on the Management and Treatment of Mucopolysaccharidosis I. Mucopolysaccharidosis I: management and treatment guidelines. *Pediatrics*. 2009;123:19-29.
38. Clarke LA. Mucopolysaccharidosis type I. In: Adam MP, Ardinger HH, Pagon RA, et al., eds. *GeneReviews® [Internet]*. Seattle, WA: University of Washington, Seattle; 2002;1993-2020. Available from: https://www.ncbi.nlm.nih.gov/books/NBK1162/.
39. Scott HS, Litjens T, Nelson PV, et al. Identification of mutations in the alpha-L-iduronidase gene (IDUA) that cause Hurler and Scheie syndromes. *Am J Hum Genet*. 1993;53:973-986.
40. Bunge S, Clements PR, Byers S, Kleijer WJ, Brooks DA, Hopwood JJ. Genotype-phenotype correlations in mucopolysaccharidosis type I using enzyme kinetics, immunoquantification and in vitro turnover studies. *Biochim Biophys Acta*. 1998;1407:249-256.
41. D'Aco K, Underhill L, Rangachari L, et al. Diagnosis and treatment trends in mucopolysaccharidosis I: findings from the MPS I Registry. *Eur J Pediatr*. 2012;171:911-919.
42. Muenzer J. The mucopolysaccharidoses: a heterogeneous group of disorders with variable pediatric presentations. *J Pediatr*. 2004;144:S27-S34.
43. Terlato NJ, Cox GF. Can mucopolysaccharidosis type I disease severity be predicted based on a patient's genotype? A comprehensive review of the literature. *Genet Med*. 2003;5:286-294.
44. Bertola F, Filocamo M, Casati G, et al. IDUA mutational profiling of a cohort of 102 European patients with mucopolysaccharidosis type I: identification and characterization of 35 novel alpha-L-iduronidase (IDUA) alleles. *Hum Mutat*. 2011;32:E2189-E2210.
45. Saito S, Ohno K, Maita N, Sakuraba H. Structural and clinical implications of amino acid substitutions in alpha-L-iduronidase: insight into the basis of mucopolysaccharidosis type I. *Mol Genet Metab*. 2014;111:107-112.
46. Ghosh A, Mercer J, Mackinnon S, et al. IDUA mutational profile and genotype-phenotype relationships in UK patients with mucopolysaccharidosis type I. *Hum Mutat*. 2017;38:1555-1568.
47. Kingma SD, Langereis EJ, de Klerk CM, et al. An algorithm to predict phenotypic severity in mucopolysaccharidosis type I in the first month of life. *Orphanet J Rare Dis*. 2013;8:99.
48. Stenson PD, Mort M, Ball EV, et al. The human gene mutation database: towards a comprehensive repository of inherited mutation data for medical research, genetic diagnosis and next-generation sequencing studies. *Hum Genet*. 2017;136:665-677.
49. Breen C, Mercer J, Jones SA, et al. Maternal mosaicism for IDUA deletion clarifies recurrence risk in MPS I. *Hum Genome Var*. 2016;3:16031.
50. Feng Y, Chen D, Wang GL, Zhang VW, Wong LJC. Improved molecular diagnosis by the detection of exonic deletions with target gene capture and deep sequencing. *Genet Med*. 2015;17:99-107.
51. Menon KP, Tieu PT, Neufeld EF. Architecture of the canine IDUA gene and mutation underlying canine mucopolysaccharidosis I. *Genomics*. 1992;14:763-768.
52. Shull RM, Munger RJ, Spellacy E, Hall CW, Constantopoulos G, Neufeld EF. Canine alpha-L-iduronidase deficiency. A model of mucopolysaccharidosis I. *Am J Pathol*. 1982;109:244-248.

53. Traas AM, Wang P, Ma X, et al. Correction of clinical manifestations of canine mucopolysaccharidosis I with neonatal retroviral vector gene therapy. *Mol Ther*. 2007;15:1423-1431.
54. Tatapudi R, Gunashekhar M, Raju PS. Mucopolysaccharidosis type I Hurler-Scheie syndrome: a rare case report. *Contemp Clin Dent*. 2011;2:66-68.
55. Wegrzyn G, Kurlenda J, Liberek A, et al. Atypical microbial infections of digestive tract may contribute to diarrhea in mucopolysaccharidosis patients: a MPS I case study. *BMC Pediatr*. 2005;5:9.
56. Nagashima K, Endo H, Sakakibara K, et al. Morphological and biochemical studies of a case of mucopolysaccharidosis II (Hunter's syndrome). *Acta Pathol Jpn*. 1976;26:115-132.
57. do Nascimento CC, Junior OA, D'Almeida V. Analysis of male reproductive parameters in a murine model of mucopolysaccharidosis type I (MPS I). *Int J Clin Exp Pathol*. 2014;7:3488-3497.
58. Eisengart JB, Rudser KD, Tolar J, et al. Enzyme replacement is associated with better cognitive outcomes after transplant in Hurler syndrome. *J Pediatr*. 2013;162:375-80 e1.
59. Moore D, Connock MJ, Wraith E, Lavery C. The prevalence of and survival in mucopolysaccharidosis I: Hurler, Hurler-Scheie and Scheie syndromes in the UK. *Orphanet J Rare Dis*. 2008;3:24.
60. Jameson E, Jones S, Remmington T. Enzyme replacement therapy with laronidase (Aldurazyme((R))) for treating mucopolysaccharidosis type I. *Cochrane Database Syst Rev*. 2016;4:CD009354.
61. Ghosh A, Miller W, Orchard PJ, et al. Enzyme replacement therapy prior to haematopoietic stem cell transplantation in mucopolysaccharidosis type I: 10 year combined experience of 2 centres. *Mol Genet Metab*. 2016;117:373-377.
62. Dickson PI, Hanson S, McEntee MF, et al. Early versus late treatment of spinal cord compression with long-term intrathecal enzyme replacement therapy in canine mucopolysaccharidosis type I. *Mol Genet Metab*. 2010;101:115-122.
63. Wang RY, Aminian A, McEntee MF, et al. Intra-articular enzyme replacement therapy with rhIDUA is safe, well-tolerated, and reduces articular GAG storage in the canine model of mucopolysaccharidosis type I. *Mol Genet Metab*. 2014;112:286-293.
64. Dierenfeld AD, McEntee MF, Vogler CA, et al. Replacing the enzyme alpha-L-iduronidase at birth ameliorates symptoms in the brain and periphery of dogs with mucopolysaccharidosis type I. *Sci Transl Med*. 2010;2:60ra89.
65. Breider MA, Shull RM, Constantopoulos G. Long-term effects of bone marrow transplantation in dogs with mucopolysaccharidosis I. *Am J Pathol*. 1989;134:677-692.
66. Dickson P, McEntee M, Vogler C, et al. Intrathecal enzyme replacement therapy: successful treatment of brain disease via the cerebrospinal fluid. *Mol Genet Metab*. 2007;91:61-68.
67. Kakkis E, McEntee M, Vogler C, et al. Intrathecal enzyme replacement therapy reduces lysosomal storage in the brain and meninges of the canine model of MPS I. *Mol Genet Metab*. 2004;83:163-174.
68. Ciron C, Desmaris N, Colle MA, et al. Gene therapy of the brain in the dog model of Hurler's syndrome. *Ann Neurol*. 2006;60:204-213.
69. Aronovich EL, Hackett PB. Lysosomal storage disease: gene therapy on both sides of the blood-brain barrier. *Mol Genet Metab*. 2015;114:83-93.
70. Simonaro CM, Tomatsu S, Sikora T, et al. Pentosan polysulfate: oral versus subcutaneous injection in mucopolysaccharidosis type I dogs. *PLoS One*. 2016;11:e0153136.
71. Frohbergh M, Ge Y, Meng F, et al. Dose responsive effects of subcutaneous pentosan polysulfate injection in mucopolysaccharidosis type VI rats and comparison to oral treatment. *PLoS One*. 2014;9:e100882.
72. Schuchman EH, Ge Y, Lai A, et al. Pentosan polysulfate: a novel therapy for the mucopolysaccharidoses. *PLoS One*. 2013;8:e54459.

SUPPORTING INFORMATION

Additional supporting information may be found online in the Supporting Information section at the end of this article.

How to cite this article: Faller KME, Ridyard AE, Gutierrez-Quintana R, et al. A deletion of *IDUA* exon 10 in a family of Golden Retriever dogs with an attenuated form of mucopolysaccharidosis type I. *J Vet Intern Med*. 2020;34:1813–1824. https://doi.org/10.1111/jvim.15868